

ROBUST BRAIN PRINT EXTRACTION USING MULTIPRONGED BRAIN STRUCTURAL IMAGING FOR SECURE BIOMETRIC AUTHENTICATION

Shaleen Bhatnagar

PhD Scholar, Department of Computer Science Engineering, Presidency University,
Bangalore, India,
shaleenbhatnagar@presidencyuniversity.com

Aditya Kishore Saxena

Assistant Professor, Department of Computer Science Engineering, Presidency University,
Bangalore, India,
adityasaxena@presidencyuniversity.in

Abstract

The brain structure is unique, hidden and comparatively stable over time than the brain's electrical signals for authentication in high-security areas. Unlike conventional biometric modalities, brain structure needs more security since the theft of the human brain's actual structure is irreversible. Issues such as scalability, uniqueness, robustness against MRI acquisition noise and template security have been insufficiently addressed by the previous methods. The useful brain structures have been segmented using an adaptive segmentation and boundary extraction algorithm. The proposed angular transformation of the original multipronged slices in the coronal, sagittal and horizontal planes, increases the effective surface area and optimizes the structural information in the brain print. Subsequent application of the irreversible layered encryption of the multipronged slices increases the effective number of final brain structural curves in the final brain print. Due to irreversibility, it is impossible to obtain the original brain structure from the final brain print. We have currently tested for 3D brain maps of 209 normal subjects. Template matching has been done through Hausdorff distance among templates. This is also the first method being reported to perform with high accuracy of 99.94% even during noisy MRI acquisition of 10% pixels. The false acceptance rate and false rejection rate in the noisy conditions are 0% and 1.1% respectively. The equal error rate is 8.4%.

Keywords: brain biometric; structural biometrics; hidden biometric; grey matter; white matter; cortical surface; template security; MRI acquisition error; portable MRI.

1. Introduction

Biometric systems utilise a person's physical or behavioural traits to identify their identification or verify that they are who they say they are Bhatnagar S. (2017). Although biometrics are thought to be a trustworthy method of authentication, there are chances it can be fabricated. Traditional biometric characteristics including fingerprints, face, hand geometry, iris, voice, signature, etc. are visible biometric traits that might be copied, stolen, or mimicked easily. The main issue with biometric systems is that once it is stolen, we can't utilize them again Bhatnagar S., et.al. (2013). When anything is hidden, however, access becomes more difficult, requiring more work and, most likely, more time to obtain the information. Forgeries and imitations become more difficult when hidden biometric traits are taken into account. When a high level of security is necessary, the use of hidden biometric features can be a good choice since they are difficult to duplicate. Some popular prevalent hidden biometrics are DNA, measurement of the electrical activity of the heart using ECG, measurement of brain signals using EEG, vein patterns, brain print, chest print, bone print, kneecaps, retinal patterns etc Bhatnagar S. and Mishra N. (2020a).

We can get 2D / 3D high-resolution medical brain images via magnetic resonance imaging (MRI) and computed tomography (CT) scans that can be utilised for biometric reasons. As no one can alter the structure of his or her brain as well as others, this approach is immune to spoofing attacks. For extracting the brain slice, the first region of interest must be selected. After getting the region of interest brain template will be created from the extracted brain slice Aloui K., et.al. (2011a). MRI gives high-resolution brain images which can be used to authenticate a person using his/her brain structural patterns. These brain structural patterns can create a unique brain print/brain code. It will be a robust biometric signature for the systems where high-level security is required.

Unlike any other biometric modalities such as fingerprints, brain structure needs more security since the theft of the human brain's actual structure is irreversible. Issues such as scalability, uniqueness, robustness against MRI acquisition noise and template security have been insufficiently addressed by the previous methods Bhatnagar S. and Mishra N. (2020b) as discussed in the next section. The proposed multipronged brain print addresses these challenges by creating a multipronged template containing optimal structural information and securing it with less processing and space complexity. The useful brain structures have been segmented using an adaptive segmentation and boundary extraction algorithm. The proposed angular transformation of the original multipronged slices in the coronal, sagittal and horizontal planes, increases the effective surface area and optimizes the structural information in the brain print. Subsequent application of the irreversible layered encryption of the multipronged slices increases the effective number of final brain structural curves in the final brain print. Due to irreversibility, it is impossible to obtain the original brain structure from the final brain print. There is a one-to-one correspondence between the subjects' brain prints as evident by their visual uniqueness among them.

The paper has been organized into 4 other sections after this section. The next section discusses various previous methods which have explored the brain structure biometrics. In section 3, we discuss the proposed algorithm with the help of five sub-algorithms. In section 4, we present the results and discussion on the results in comparison to the previous methods. Finally in section 5, we conclude with prospective future extension of this work. Let us now explore previous approaches which have tried to establish brain structure as a strong biometric candidate.

2. Literature Review

An ideal biometric template should not be simpler to steal, and it shouldn't be left exposed. These conditions are addressed by hidden biometrics. It can be characterised as a particular class of biometrics whose goal is to take into account a person's behavioural and physical traits that are not readily apparent. It makes use of data that is typically applied in the healthcare arena. These strategies are effective against spoofing. Our goal is to determine whether or not human brain scans can also be used for verification. Gyrus and sulcus patterns provide the brain code or brain print. A distinctive trait results from brain growth in the skull. According to newly found Jumping genes, even twins do not grow their brains in the same way. In 2015, Wachinger et al. made an effort to categorise people based on their neuroanatomical characteristics. A novel mathematical model for anatomical data structure analysis from public brain databases of MRI scans to create a brain print with 99.8% correctness in identifying the people has been attained Wachinger C., et.al. (2015). It may be inferred from the research of Wachinger et al. (2015), Dubois & Adolphs (2016), Finn et al. (2017), and Valizadeh et al. (2018) that the structure of the brain is distinct. In two different ways, texture analysis and shape & structure analysis, a few researchers have explored the idea of employing brain codes as biometric traits Wachinger C., et.al. (2015); Dubois J. and Adolphs R. (2016); Finn, et al. (2017); and Valizadeh, et al. (2018). Authors Alouil K., et.al. (2011b) employed a single slice from a volumetric scan of an MR for texture analysis. They specifically extracted textural information from two-dimensional pictures of cortical folds using the 1D Log-Gabor transform. They created a binary template that served as their brain code. Using Hamming distance, they verified the brain code. They Alouil K., et.al. (2011b) used only one slice of a volumetric picture from an MR to analyse the shape and organisation of a collection of cortical and subcortical regions. Particularly, the ellipse that defines the brain is used to extract brain form attributes. Afterwards, they produced a vector representation that expressed the structure of the brain. The estimation of resemblance was verified using a range normalised Euclidean distance. To extract grey matter from an input brain image, authors Chen, et al. (2014) presented a brain segmentation algorithm. Then, for brain code verification, a matching method based on alignment was created. To normalise the images and conduct brain recognition, authors Takao, et al. (2015) employed a voxel-based morphometric technique. Principal component analysis was used for feature extraction. They employed the Euclidean distance between both the image pairs for verification. Geometrical characteristics of the brain, such as structure, can be utilised to determine inter-individual variations in brain structure and to confirm the identity Alouil K., et.al. (2011a). Considering various previous works let us explore the challenges, opportunities and our propositions to work in this area of research.

2.1. Challenges, Opportunities and Propositions

The brain is a 3D structure, which poses a challenge of complex cubical image data to be handled by the processor and requires large memory. Structural features involving complete brain volume and cortical surface area Alouil K., et.al. (2011a); and Bassi M., et.al. (2018) need improvement. The whole 3D volume may not be required to be loaded into the memory but the analysis can be done slice by slice and summation later. Single slice selection algorithms Wachinger C., et.al. (2014); Maheshwari S., et.al. (2016); and Bassi M., et.al. (2018) choose a slice of a specific voxel based on a secret key but the unidimensional slice does not have optimal brain structural information required to make the template scalable. This also restricts the template to containing structural information from only one plane. Thus, we propose to make the selection of specific slices in all the dimensions. We propose a multipronged point selection inside the 3D brain. The orthogonal slices at this point in coronal, sagittal and horizontal planes are chosen for biometric template extraction. These slices are to be processed to

extract brain curves which are in the form of sulci and gyri. Brain curves have been extracted in Maheshwari S., et.al. (2016) and an artificial polygon has been created by approximating the edges of the polygon using the brain curves. Due to the limited number of edges in the polygon, matching of exact coordinates of brain curves may not be possible in some cases and will lead to a finite set of unique brain prints limiting the scalability of the system. The brain curve information must not be stored explicitly but as a transformed brain print which is irreversible to extracting actual brain shape and curves Aloui K., et.al. (2018). But again, a single slice limits scalability and thus structural information in all planes must be used. We envision adding two more layers of security. First, we use novel angular slices which are inclined to the coronal, sagittal or horizontal planes instead of original orthogonal slices. This may enhance the brain biometric template due to the larger traversal of the brain structure. This also ensures the transformation of the original brain slices in natural planes to secret angular planes but still, the actual brain structure is there. It is also important to apply strong and irreversible encryption over the brain print. We have devised a low-complexity layered encryption method to create a unique brain print from the angular slices and create a transformed brain print. In the next subsection, we describe the methodology to select the multipronged point and create the proposed robust multipronged brain print.

3. Proposed Work

The human brain's structural information has been used to create biometric templates by various approaches which have been discussed with respective pros and cons in the previous section. These approaches lack robustness which motivated us to formulate the challenges and look for possible solutions by exploiting the opportunities available for the robustness development in these methods. Figure 1 visually describes the process flow of brain print registration for biometric model training on the left side and the testing phase to check query brain print and identify the subject for authentication.

Sr. No.	Symbol	Use
1.	BM	3D brain map in NII
2.	U	User ID
3.	S	Secret Key
4.	PNgen	pseudorandom number generator
5.	K	The generated secret seed for PNgen
6.	(px, py, pz)	The multipronged point 3D coordinates
7.	N_SLC_COR N_SLC_SAG N_SLC_HOR	Normal Brain Slice in all the three planes viz. Coronal, Sagittal and Horizontal planes respectively
8.	A_SLC_COR A_SLC_SAG A_SLC_HOR	Angular transformed brain slice in the three planes
9.	F_SLC_COR F_SLC_SAG F_SLC_HOR	Segmented and ROI extracted angular transformed Brain Slice in the three planes
10.	xshift, yshift, zshift	Angular Shifts in three planes respectively
11.	i, j	Row and column index respectively
12.	Slice	Intensity matrix of a slice
13.	L1, L2, L3	Three layers of multipronged brain slices input for layered encryption
14.	M	Layered encrypted multipronged template

Table 1. Abbreviations, Symbols and their uses in this paper

3.1. Multipronged 3D point selection

Complete 3D brain map in Neuroimaging Informatics Technology Initiative (NII) format (BM) is taken as input along with a unique user ID (U) and a secret key (S) from the registering user. The secret key and user ID are used to generate a seed for a pseudo-random generator for the whole system. This key is used as the seed of a pseudo-random number generator. A 3D point is selected at random anywhere in the 3D brain mass using this seed.

3.2. Angular Brain print Creation Method

Three slices, one in each plane, are extracted named as Coronal plane (N_SLC_COR), Sagittal plane (N_SLC_SAG), and Horizontal plane (N_SLC_HOR) passing through this point with coordinates (px, py, pz). Now we generate secure angular deviations (xshift, yshift, zshift) from the secret key in all planes respectively. Each of these planes at a multipronged point is transformed with respective angular deviation. Angular interpolation is done to generate angular transformed planes respectively as explained in step 6 of algorithm 1. The visual model of the angular transformation of the coronal slice has been visually represented in figure 2. Due to a secret angle of inclination from the actual brain orthogonal axes, these slices cover larger brain areas and thus higher number of structural curves in comparison to the normal slices. As evident from figure 2 the surface area of the angular transformed slice (shown in red) is always larger than the normal slice (shown in blue) proving the hypothesis.

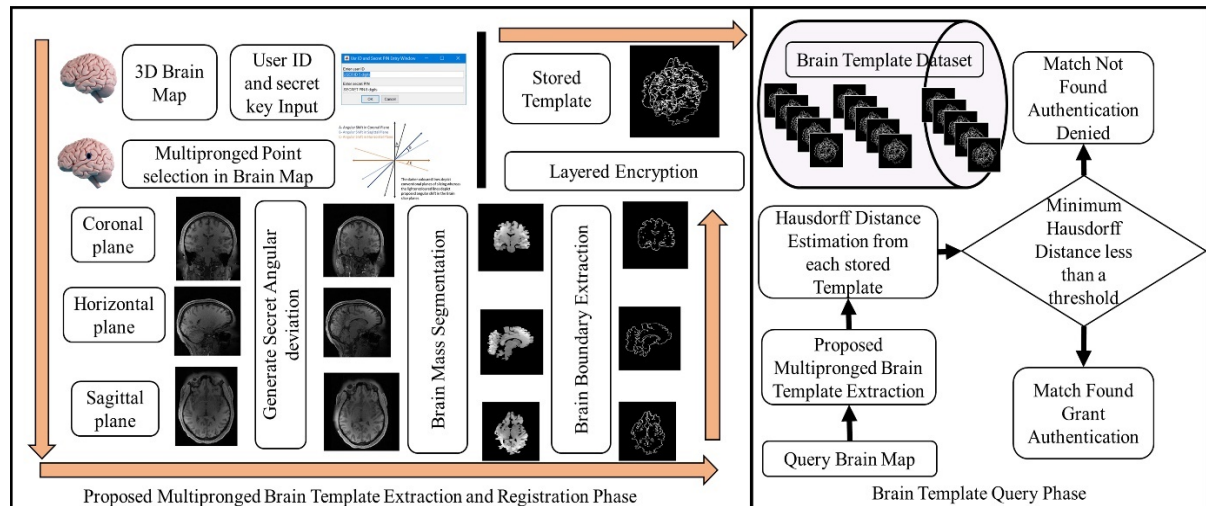


Fig. 1 Process flow schema of the proposed multipronged brain print extraction, registration and query phase

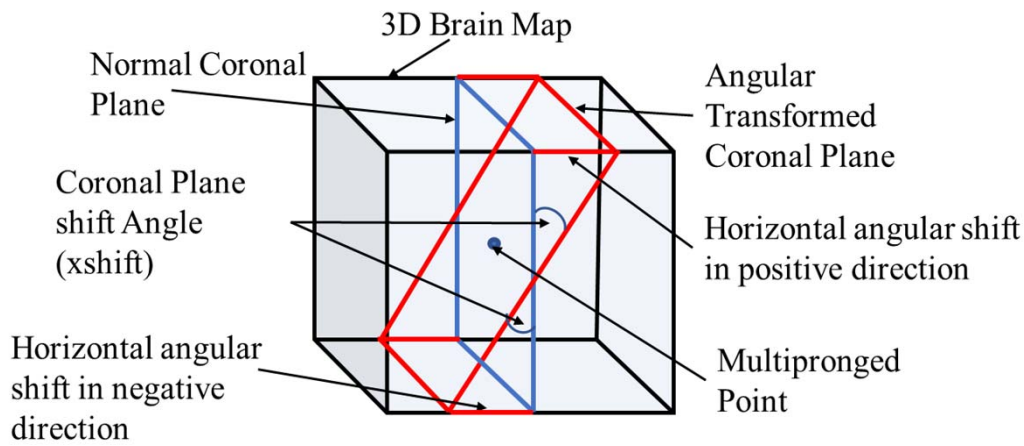


Fig. 2. Visual Model of the proposed Angular transformation of normal brain slice planes

Algorithm 1: Proposed Secure Optimal Brain Structural Biometric Cube

Input:

1. 3D brain map in NII format (BM)
2. User ID (U) and secret key (S) of the user

Multipronged_brain_brain print_extraction(BM)

1. Generate secret key $K = \text{mod}(U, S)$
2. Set pseudorandom number generator (PNgen) seed = K
 - a. PNgen = multiplicative lagged Fibonacci generator seeded with K
3. Multipronged point coordinates in brain map (BM) using PNgen
 - a. $(px, py, pz) = \text{Generate_multipronged_point}(\text{BM})$
4. Slice extraction in following Orthogonal planes at multipronged point (px, py, pz)
 - a. Coronal plane (N_S LC_COR)
 - b. Sagittal plane (N_S LC_SAG)
 - c. Horizontal plane (N_SLC_HOR)
5. Secret angular deviation is generated from the secret key different for each plane using PNgen
 - a. $[xshift, yshift, zshift] = \text{Generate_angular_deviation}()$
6. Create a brain print with a respective angular deviation
 - a. For each plane
 - i. For each $[i,j]$ pixel in each plane

1. Find [i,j] angular pixel corresponding to the [i,j] orthogonal plane pixel by estimating the number of shifts either in right or left direction of the orthogonal plane
2. If shift_angle ≥ 0
 - a. Create a range_shifts using [+shiftangle, -shiftangle]
3. Else if shift_angle < 0
 - a. Create a range_shifts using [-shiftangle, +shiftangle]
4. Choose pixels [i,j] of the angular shifted plane as (px+(range_shifts))
- ii. Repeat for each plane to create an angular slice in each plane as A_SLC_COR, A_SLC_SAG, A_SLC_HOR
7. Segmentation of brain mass, Extraction of brain boundary and region of interest (ROI) brain and its centre of each slice
 - a. call F_SLC_COR=brain_segment(A_SLC_COR)
 - b. call F_SLC_SAG=brain_segment(A_SLC_SAG)
 - c. call F_SLC_HOR=brain_segment(A_SLC_HOR)
8. Apply Layered Encryption over segmented angular transformed orthogonal slices
 - a. Multipronged_brain_brain print = Layer_encrypt(F_SLC_COR, F_SLC_SAG, F_SLC_HOR)

Output:

Secure Multipronged brain print

3.3. Brain Curves Extraction

The MRI images given as input have the skull, brain and cerebrospinal fluid. It may also have the upper part of the spinal cord and other brain areas which we are not interested to create the biometric templates. It is essential to segment the brain of this input image and discard the remaining part in the image. We use image thresholding to extract the brain from the head MRI image. We find the maximum intensity level in the image to know the white matter. An intensity map is created based on the maximum level with contour, surface and color. We then apply global thresholding rules to ignore certain parts of the image such as low levels (CSF & air) and high-intensity levels (skull & other hard tissues). We also ignore spatially low positions (below brain mass). We then erode the thick layer to dissolve the thin surrounding tissues. Now to isolate the brain mass we apply the global image threshold using Otsu's method creating a binary image having the brain mass. By analyzing the connected region properties, we keep the biggest area and discard others. Inside this biggest area, we again apply thresholding to separate grey and white matter. Now we estimate the boundary of the brain by detecting the edges of the grey matter denoting the sulci and gyri structures. This binary image of the detected brain images is further used for the creation of the brain print. The algorithm 2 gives the detailed steps for segmentation of the brain mass, extraction of brain boundary and region of interest from the multipronged brain slices.

Algorithm 2: Segmentation of brain mass, Extraction of brain boundary and region of interest (ROI) brain and its centre of each slice

Brain_segment(Slice)

1. Segmentation
 - a. Maximum intensity level in the image to know the white matter
 - i. max_level = max(Slice);
 - b. Apply thresholding and ignore certain parts of the data
 - i. For each pixel of the slice with
 1. (intensity ≤ 200) make it to 0 to ignore low levels (CSF & air)
 2. (intensity $\geq \text{max_level}/2$) make it to 0 to ignore high levels (skull & hard tissues)
 - c. Erode thick layer (dissolve thin surrounding tissues) using structuring element for erosion [3 7 7]
 - d. Isolate brain mass by global image threshold using Otsu's method and make a binary image which has the brain mass with a value more than the intensity threshold
 - e. Estimate connected region properties for the number and size of areas
 - f. Shortlisting the biggest connected area
 - g. Discard remaining image areas
 - h. grow back main region (brain mass)
 - i. return the segmented brain
2. Extraction of brain boundary

- a. Inside segmented brain mass
 - b. Run thresholding
 - c. Partition brain mass with threshold lev into 3 regions
 - i. Type 1 outside brain (head/air)
 - ii. Type 2 gray matter
 - iii. Type 3 white matter
 - d. Estimate boundary by scanning segmented brain by creating boundaries where the pixel type changes
 - e. Store all boundary pixels as 1
 - f. Return binary boundary extracted binary image
3. ROI extraction
 - a. Search for the first non-zero row from the top, and bottom
 - b. Search for the first non-zero column from left and right
 - c. Extract useful brain mass boundary between these rows and columns
 - d. Return ROI extracted brain binary image
 - e. Centre estimation and padding for merging

3.4. Layered Encryption

Encryption is the process which hides an important secret by transforming it into another form. The decryption process is done to extract the secret from the transformed brain print. We use the proposed one-way layered encryption here for merging the angular slices. This step is essential to secure the actual brain curves present in the slices. This step solves two important problems, the first is to reduce the amount of data by creating a final binary merged slice of size 320 by 320 pixels and the second is to create an irreversibly transformed brain print with higher number curves which have been modified from their actual shapes. We use the binary ROI extracted images for merging as per the steps followed as listed in Algorithm 3.

Algorithm 3.

Layer_encrypt(L1, L2, L3)

1. Mid-point estimation
 - a. Find spatial mid-points of ROI extracted images
2. Pad the image with zeros to equalize all brain slices L1, L2 and L3
3. Repeat for each row i of L1
 - a. Repeat for each column j of L1
 - i. $M[i,j] = \text{OR}(L1(i,j), L2(i,j), L3(i,j))$

Here OR() is the bitwise OR logical operation with output logic high (1) with at least one high (1) input.

3.5. Brain print Matching

Pixel-by-pixel image difference assessment is not sufficient to differentiate between the brain curves. In case of image processing attacks, or noisy medical images the curves will not be in the same place or may have poor clarity. So, the matching process has to be intelligent enough to differentiate between true and false matches. The step-by-step process of brain print matching has been given in algorithm 4. Previous methods have used correlation as a matching strategy which is also useful in the case of grayscale images but since we have final brain prints in binary form and there are various curves and polygons present in the final multipronged brain print. We use Hausdorff Distance (HD) for matching the brain prints. The brain prints stored in the database must have sufficient HD among themselves to ensure the scalability of the process. The matching is guaranteed to have a minimum HD between any two brain prints with the ideal HD to be 0. Even in the case of noises, the HD of the matched brain print should be near 0. Hausdorff distance is the maximum distance of a set to the nearest point in the other set. More formally, Hausdorff distance H from set A to set B is a function, defined as in Eq. (1) as follows

$$H(A, B) = \max_{a \in A} \{ \min_{b \in B} \{ d(a, b) \} \} \quad (1)$$

where a and b are points of sets A and B respectively, and $d(a, b)$ is any metric between these points; we use the Euclidian distance between a and b . We exploit the image matching capability of HD, used for applications such as image analysis, visual navigation of robots, etc. The Hausdorff metric will serve to check if a brain print image is present in a test image; the lower the distance value, the best the match. It can match specific structures in two images even if they are not spatially aligned with each other using the steps as listed in algorithm 5. We envision finding successful matches even in presence of noise such as MRI acquisition errors.

Algorithm 4: Brain print Matching algorithm

Input: query_brain_map

Match_query_brain_map(query_brain_map)

1. Query_brain print=Multi pronged_brain_brain print_extraction(query_brain_map)
2. For each brain print k in stored_dataset (k is the index of stored brain prints)
 - a. $HD(k)=\text{Extract_Hausdorff_distance}(\text{brain print}_k, \text{Query_brain print})$
3. Find minimum Hausdorff distance and index [min_HD , index] = minimum(HD)
4. If $\text{min_HD} \leq \text{threshold}$ ($HD \leq 10$)
 - a. Return Match Found with registered subject k
 - b. Authentication Approved
5. Else
 - a. Return No match found
 - b. Authentication denied

Algorithm 5: To extract Hausdorff distance between two images of the same size using Euclidean distance as the distance metric

Input: Two images A and B

Extract_Hausdorff_distance(A, B)

1. $h = 0$
2. for every point a_{ij} of A, i denoting row and j column
 - a. $\text{shortest} = \text{Inf}$;
 - b. for every point b_{xy} of B, x denoting row and y column
 - i. $d_{ijxy} = \text{Euclidean_distance}(a_{ij}, b_{xy})$
 - ii. if $d_{ijxy} < \text{shortest}$ then
 1. $\text{shortest} = d_{ijxy}$
 - c. if $\text{shortest} > h$ then
 - i. $h = \text{shortest}$
3. return h

In the next section, we present the results of the implementation of the proposed brain structural brain print creation. We also discuss various performance parameters which prove the robustness of the proposed system.

4. Results and Discussions

The target data for the proposed method is the brain imaging data obtained from portable brain scans. However, as the research is ongoing in that area so it is expected to receive some promising datasets of brain imaging from portable devices soon for public research. Meanwhile, to validate the proposed method, we chose the Human Connectome Project, WUMinn HCP Data having 1200 normal subjects Rosen V. and Toga W. (2010). This dataset is a collection of structural unprocessed T1 and T2 weighted 3D brain scans in the Neuroimaging Informatics Technology Initiative (NIFTI) format. The metadata in *.csv format related to the scan acquisition is also available which is necessary to construct the field maps. We utilized MATLAB v2021b for the implementation of the proposed algorithm. We present the detailed results and analysis for the development of the proposed multipronged brain biometric brain print creation. We trained the proposed method by registering brain maps of 180 subjects and tested 100 subjects out of which 71 subjects were known to the trained system and the remaining 29 were unknown. All of these were randomly chosen from the HCP dataset. The algorithm has been run on an Intel Core i7 system with 16 GB of RAM, however, the actual requirement of the runtime memory and processing unit is very less as proven in the algorithm complexity section.

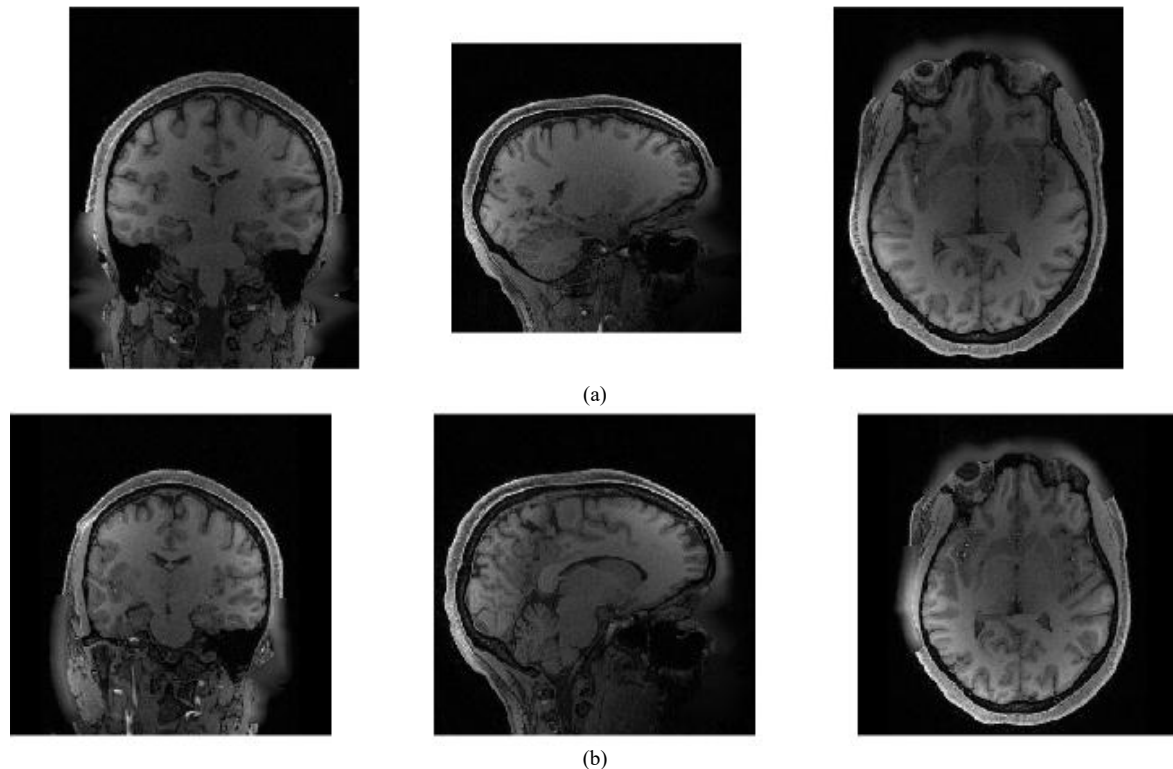


Fig. 3. (a) Normal (b) Angular transformed Brain slices in coronal, sagittal and horizontal planes at the multipronged point

4.1. Normal and Angular Transformed Multipronged Slices

The 3D brain mass is scanned for specific orthogonal slices in coronal, sagittal and horizontal planes at the multipronged point as shown in figure 3 (a). These original slices are angular transformed and interpolated using the proposed algorithm as shown in figure 3 (b). It is important to note here that these are entirely different in structure from normal slices which also ensures the hidden identity of the actual traditional orthogonal slices useful for other medical applications.

4.2. Segmented and Boundary Extracted Multipronged Slices

The brain images contain other cranial parts also other than brain mass. It is important to extract only the brain mass for the extraction of actual brain structure. The segmented brain mass has a 2D structure as shown in figure 4 (a), previous methods have used such brain mass for brain print generation. Instead of using the brain structure, we envision using the brain boundary since the inner area (white matter) is not exactly required and will only make the final data structure of large size. To keep the brain print in binary format, with the minimum number of pixels and all of them denoting the brain structure only, we use the boundary extraction method to separate the brain mass from the surrounding area. Figure 4 (b) shows the boundary extracted images of the multipronged slices.

4.3. Generation of Layered Encrypted Multipronged brain print

The angular transformed slices contain the brain data which cannot be directly stored due to security reasons. It has brain structural information and to increase the safety of the brain print it is necessary to encrypt the information and minimize it for storage. We apply the proposed layered encryption to produce a secure brain print as shown in figure 5. This encrypted brain print is created by the overlapping of ROI extracted and padded multipronged slices. As visible in figure 5, it is impossible to extract the original structure of the brain present in multipronged slices since this overlapping is irreversible. It is important to note that the number of curves present in this final brain print is more than any other method in the literature. Also, the arrangement of curves is unique as we hypothesized for different subjects.

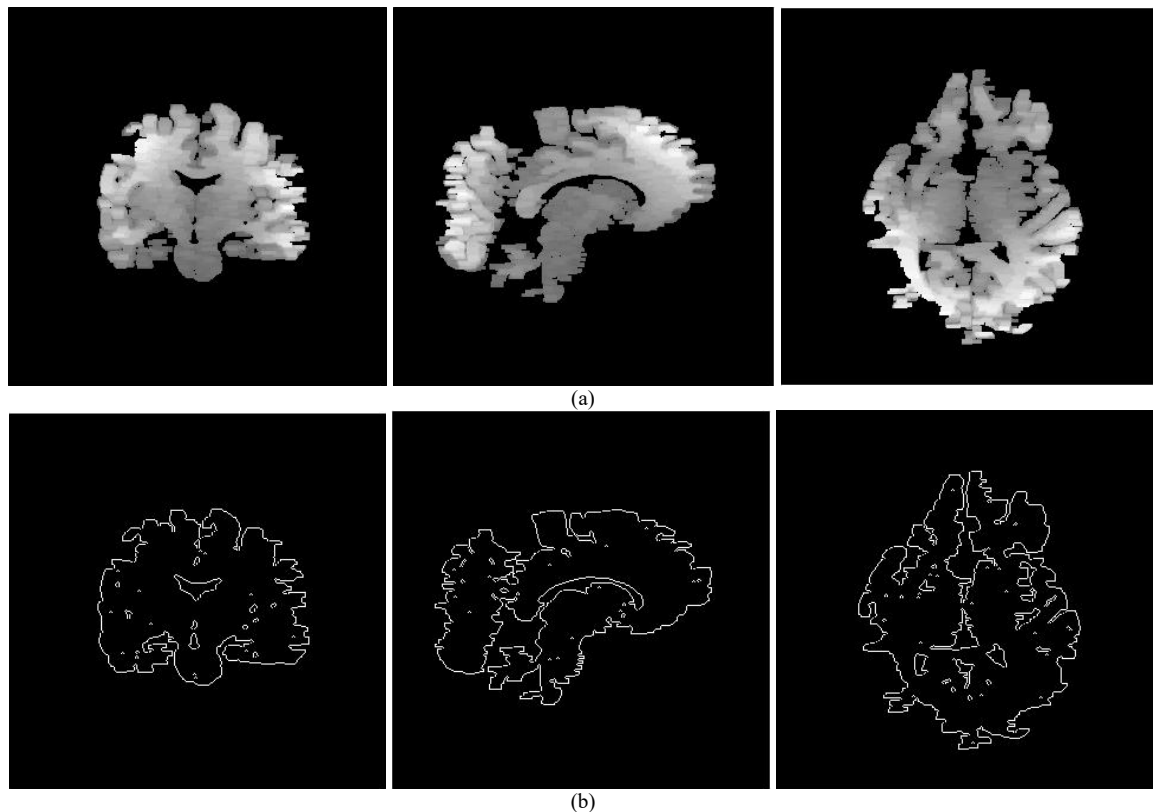


Fig. 4 (a) Segmented (b) Boundary extracted angular transformed brain slices in coronal, sagittal and horizontal planes at the multipronged point

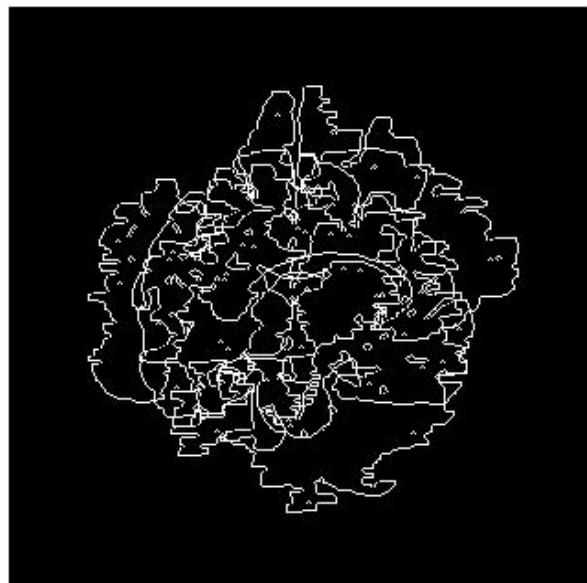


Fig. 5. Resultant Multipronged Brain Biometric Brain print

4.4. Query and Distance Matching

We generated a query engine to test the proposed biometric model trained by 180 subjects as discussed earlier. The query engine works to detect the accuracy of the system by estimating false positives and false negatives. We run a total of 100 queries out of which 71 are known subjects while 29 are unknown subjects. The known subjects' brain prints are available in the trained model while the unknown subjects' brain prints have been created in run-time during query. Genuine registered subjects' brain prints are sufficiently different from each other and the Hausdorff distance between them is more than 13.5 units which have been set as the matching threshold. The minimum HD between any two brain prints is less than this threshold is obtained then only a successful match is declared as shown in figure 6 the query template matches with subject serial number 24 only. The performance

of the system has been evaluated in the terms of false acceptance rate (FAR), false rejection rate (FRR), equal error rate (EER) and accuracy as defined in Aloui K., et.al. (2011a). The false positives of the system are 0 which makes FAR also zero. There are no false negatives so it is also 0 thus FRR is also zero. In the worst case when secret keys are the same for all subjects, or someone knows the other subject's ID and password, even then in absence of the subject's brain map, authentication will not be approved, FAR and FRR are both 0 even in this case.

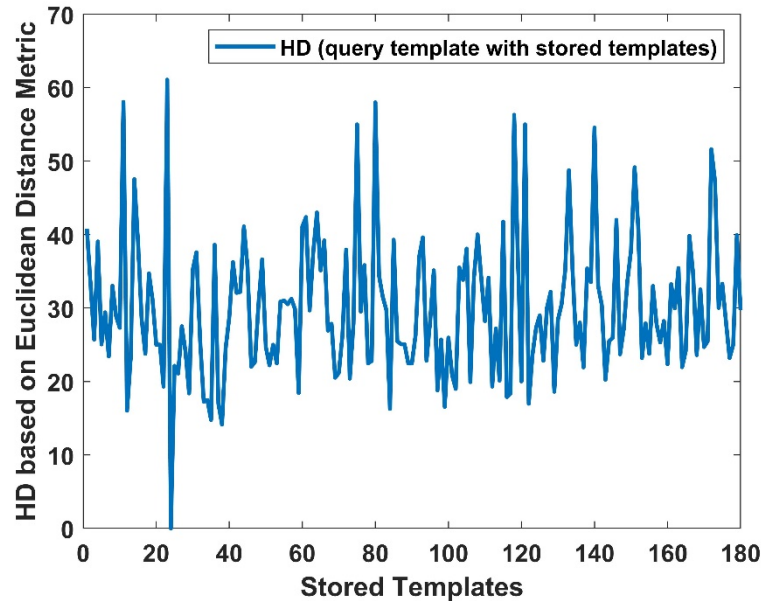


Fig. 6. Brain print matching result with successful match with the subject with serial number 24 since the HD is less than threshold 13.5 for this only.

4.5. Robustness of the Brain print

To ensure that the brain print is secure and robust enough to be used for practical differentiation among human subjects, we analyze the generated brain cube brain print on the following three parameters.

4.5.1 Irreversibility to Recreate Actual Brain Structure

Due to the use of one-way layered encryption, the three angular transformed planes of the brain are merged into a single plane. Even if the attacker gets the final template, it is impossible to generate the original planes having the brain structural information cannot be generated again from the multipronged brain print as shown in figure 5.

4.5.2 Brain print Uniqueness and Scalability

Individual brain slices have been proved to be unique due to the unique structures of sulci and gyri. We choose a multipronged point in the brain mass and merge them using layered encryption to generate a brain print. The final brain print is expected to be unique for each subject. The visual differences among the various stored brain prints can be seen in figure 7. The difference among the templates has been analyzed to estimate uniqueness among the biometric brain prints of different subjects. Distance between pair of brain prints of any two subjects in terms of Hausdorff distance has been estimated. We consider two cases, the best case when all the subjects have unique secret keys, and the worst case when all the subjects have the same secret keys. We estimated Hausdorff distances among all the brain print pairs in the dataset. The image representation of Hausdorff distance among the 209 brain prints for the worst case has been shown in figure 8. It represents that the brain prints are sufficiently different from each other with the majority of the unmatched distances >15 in the green region. The performance of the system in the ideal scenario with best case and worst case is shown in table 1. In ideal MRI estimation conditions without any acquisition noise, for different subjects' brain prints comparison, the HD is always more than 13.5 units. The red-colored bar in a histogram in figure 9 represents the correct matches and the blue bars show the unmatched comparisons. Clear separation in the histogram figure 9 between matched and unmatched brain prints indicates that the templates are highly unique, which induces the scalability of the system to ensure its future application to develop a global biometric with a large number of subjects.

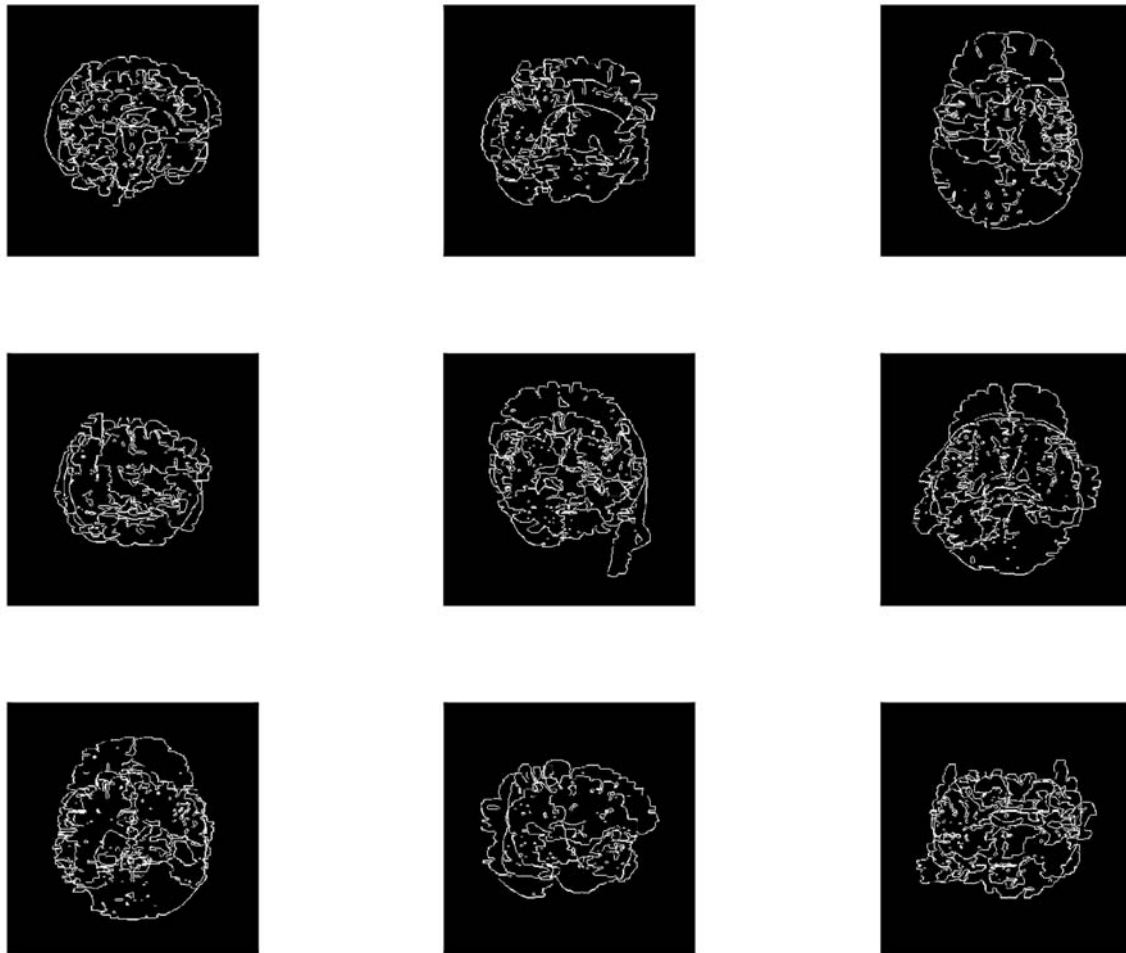


Fig. 7. Sample binary multipronged brain prints stored after registration

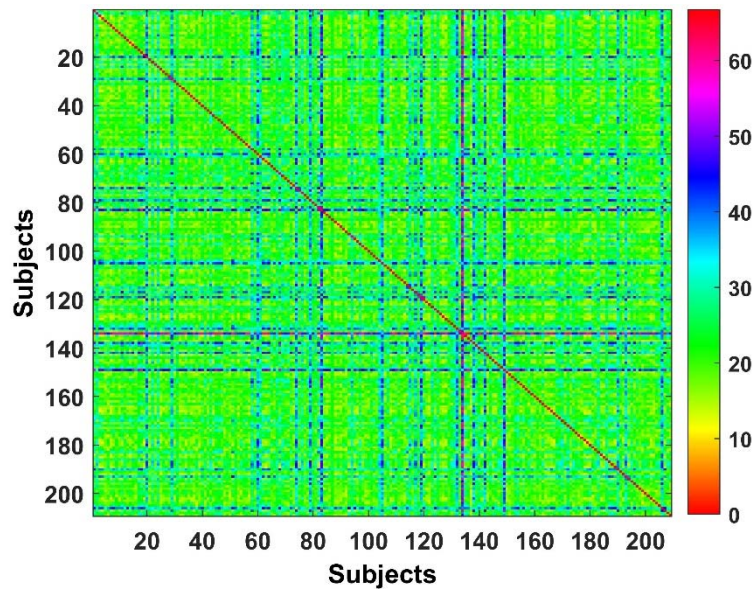


Fig. 8. Image representation of Hausdorff distance among the 209 brain prints for worst case, the figure represents that the brain prints are sufficiently different from each other with a majority unmatched distances >15 in the green region

4.5.3 Consideration of MRI acquisition noise

MRI acquisition is seldom 100% repeatable. An error of about 5 to 10% is expected in the intensities level while MRI estimation. Previous methods have not considered this fact while brain print generation as well as accuracy estimation. Method Valizadeh, et al. (2018) analyses the brain print against a noisy scenario but the F1 score degrades. We embed artificial intensity estimation noise on 5% and 10% of the pixels in the acquisition of the query template before template extraction to analyze performance under the presence of noise. The results of matching in this scenario are mentioned in figure 10, table 2 and table 3. Figure 10 (a) and (b) show the FAR and FRR plots in presence of 10% noise of 5% respectively. The intersection point of these plots is at 8.4% and 2.8% denoting EER at specific thresholds. The results have been summarized in table 2. Table 3 represents the relationship between FAR and FRR, we choose the system threshold as 13.5 to minimize FAR to 0. At this threshold, the system shows 99.94% accuracy for matching.

S. No.	Parameter Name	Value	Significance
1.	Average Correlation	0.11	This value depicts the average matching among the stored brain prints. The lesser the average correlation more robust the approach.
2.	Mean Hausdorff Distance (Worst Case)	24.1 Units	This value depicts the average Hausdorff distance among the stored brain prints depicting that each brain print differs on average and does not match with others more than this on average. (Here, the brain print has not been correlated with itself.)
	Mean Hausdorff Distance (Best Case)	35.2 Units	
3.	Minimum Hausdorff Distance between any unmatched pair (Threshold)	13.5 Units	It is the average of the minimum Hausdorff Distance between any unmatched pair which is used by the proposed matching system to decide the matching threshold. Any HD between two templates below this HD is only considered a successful match.
4.	Average brain prints processing time	0.91 sec	This depicts the processing time required for the creation of the proposed biometric brain print from the 3D brain map. Time less than 1 sec depicts the real-time nature of the proposed algorithm.
5.	Average per brain print matching time	0.01 sec	This depicts the average processing time required for matching a query brain print to one stored brain print to determine the best match.
6.	The complexity of angular transformation and brain print creation	$O(n^2)$	Size of each normalized brain slice ($n \times n$) pixel, we use 3 slice planes and $n \gg 3$
7.	The complexity of brain print matching	$O(Nn^2)$	Here N is the number of registered subjects.

Table 1. Performance metrics for the worst-case scenario of the proposed method

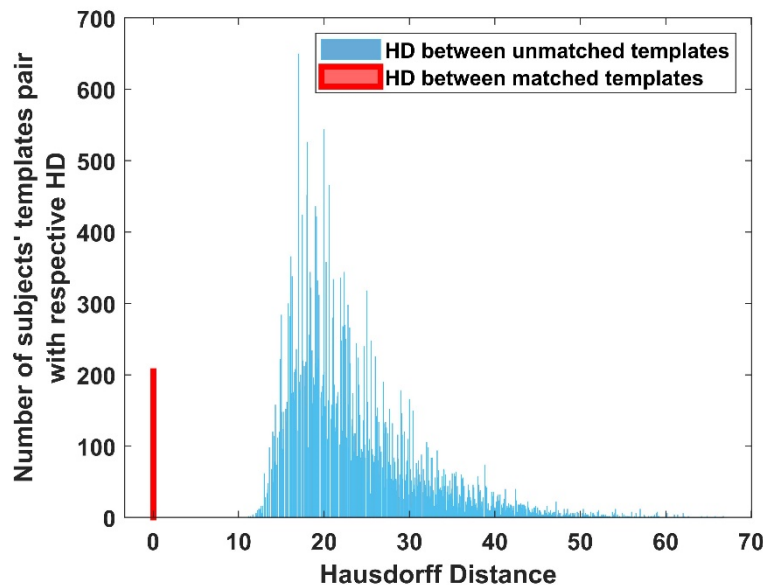


Fig. 9. Worst-Case distance estimation with Hausdorff distance for unmatched is more than 10 units

	MRI Loss 0%	MRI Loss 5%	MRI Loss 10%
EER	0	2.8	8.5
Threshold	13.5 OR LESS	13.5	14.3

Table 2. EER and HD threshold in case of MRI image acquisition error while query matching

Threshold	FAR	FRR	Accuracy
4.1	0	1	99.5
4.2	0	.98	99.5
5.4	0	.88	99.5
6.1	0	.76	99.6
7.3	0	.49	99.7
9.5	0	.28	99.8
10.6	0	.22	99.9
13.5	0	.11	99.94
13.7	0.03	.09	99.93
14.3	.08	.084	99.9
15.1	.3	.08	99.8
18.1	.7	.07	99.6
19.7	1	.04	99.4

Table 3. FAR and FRR while MRI imaging error of 10%

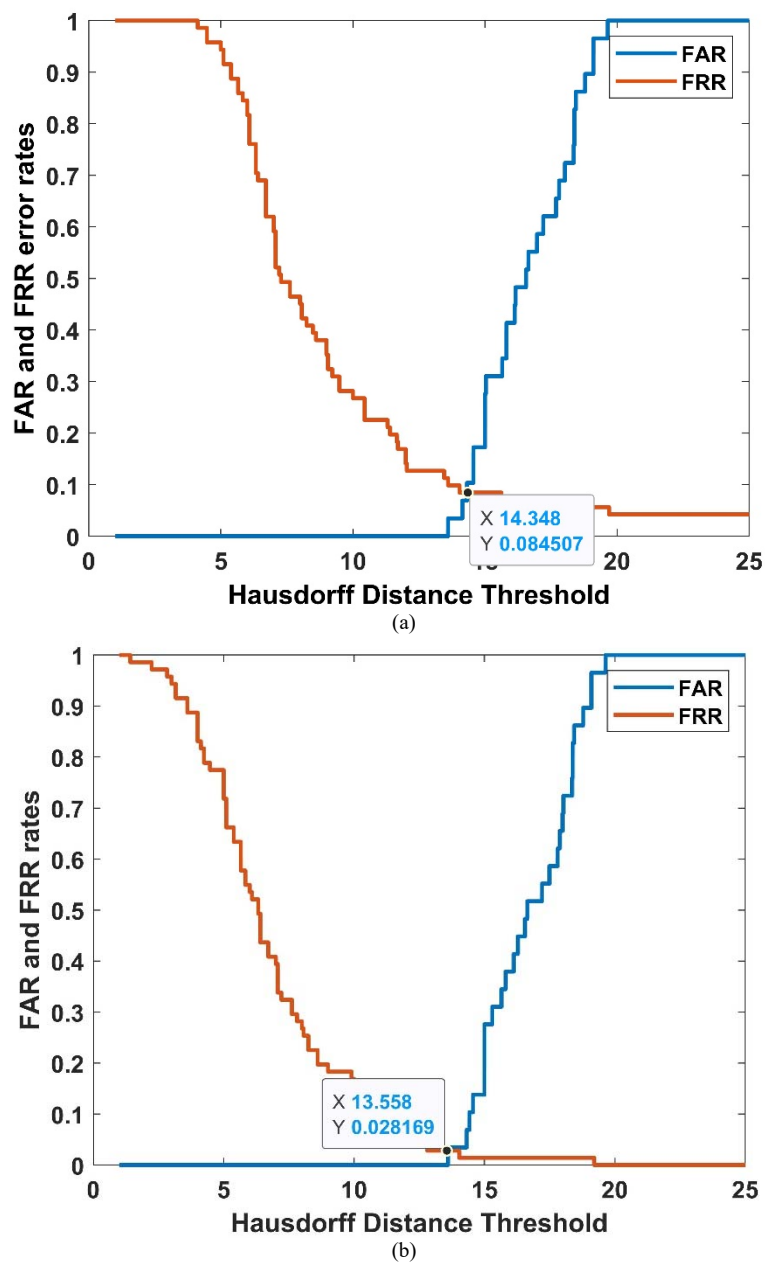


Fig. 10. FAR and FRR comparison for various Hausdorff Distance over two different MRI scanning intensity estimation error rates of (a) 10% and (b) 5%. The intersection points of these plots show EER on the Y axis and respective Hausdorff distance threshold on the X axis.

4.6. Comparison with Previous methods

Use of Cortical Surface: Four different cortical surfaces have been used for biometric template generation by converting them into 2D cortical fold maps surface images in Aloui K., et.al. (2018) and meshes which have specific shapes in Wachinger C., et.al. (2015). The results are inspiring but the internal structure of the brain may give additional structural insight without any extra processing Aloui K., et.al. (2018) as done by us.

Complete brain's volumetric analysis: Complete brain volumetric and surface area analysis has been done for the complete brain to estimate various features which increase processing and matching time Valizadeh, et al. (2018). Our proposed algorithm shows that using the limited number of slices in all the planes shows equal accuracy.

Brain structure representation through single slice: The limited structure of the brain is extracted as a single brain slice Aloui K., et.al. (2011a) or brain curves by skeletonizing the white matter Bassi M., et.al. (2018) after segmentation and an approximate elliptical structure. The segmented coronal slice selected in a secure method has been transformed into 16 polygon vertices so have limited scalability Maheshwari S., et.al. (2016). Single slice geometrical features have limited brain structural information. The scalability of this method for many subjects is doubtful since many subjects may have this ellipse with the same geometrical parameter Aloui K., et.al. (2011a). Also, robustness is limited since the 3D brain has not been considered to maximize the structural information Bassi M., et.al. (2018). A fixed slice number 128 has been used for feature extraction and matching which makes the approach vulnerable to attacks Chen, et al. (2014).

Approaches	Aloui K., et.al. (2018)	Wachinger C., et.al. (2015)	Valizadeh, et al. (2018)	Aloui K., et.al. (2011a)	Bassi M., et.al. (2018)	Aloui K., et.al. (2012)	Maheshwari S., et.al. (2016)	Proposed
Parameters								
Accuracy %	99.6	99.9	100 but drops with noise since the F1 score is 0.6	98.25	100 but only in the ideal condition	99.46	NA	99.94
Brain Imaging Errors Considered	No	No	Yes	No	No	No	No	Yes
EER	2.9	NA	NA	NA	NA	2.13	NA	2.8
Number of subjects	220	700	191	210	100	416	100	209
Irreversibility	No	No	No	No	No	No	Yes	Yes
Template Security	No	No	No	No	No	No	Yes	Yes
3D brain structure utilization	Yes, only Surface	Yes, only Surface	Yes, the whole brain	No, single horizontal slice	No	Yes, single slice number 128	No	Yes
Template Storage	Gabor features	Shape descriptors 9KB	Volumetric Measures	Ellipse geometrical features	Image	Images	Polygon vertices	Binary Image <4KB
Processing and Matching time	Not reported but high	Not reported but Medium	Not reported but High	Not reported but Medium	0.1 sec and 0.01 sec	Reported high	Not reported but medium	0.91 sec and 0.01 sec
Uniqueness and scalability tested	No	No	No	No	No	No	No	Yes

Table 4. Performance comparison of the proposed method in the case of MRI imaging errors consideration (10%) with previous methods

The template has reference to the original brain structure: Approach Chen, et al. (2014) works on the principle of grey matter extraction and its matching among the subjects. The template remains in its original structural form which is not secure again template theft Chen, et al. (2014). The actual brain curves are there in the final image stored as the template so security issues are there Bassi M., et.al. (2018). The final features still directly represent the actual brain structural features which may cause security issues Aloui K., et.al. (2018).

The attribute-wise comparison between the proposed method considering the MRI intensity estimation noise and previous methods has been done in table 3. It can be seen that very few approaches have dealt with MRI acquisition noise and even with the noise the accuracy of the proposed approach is comparable to or higher than all others. Very few methods are scalable to make a global biometric and the security of the final template has not been considered.

4.7. Requirement for low-cost and portable MRI system

The main withholding for the proposed work is the complex imaging of the brain specifically through MRI. However, recently some low-cost and portable brain imaging equipment have been tested which may induce the mass use of brain print as biometrics for authentication. The Hyperfine Swoop™, the world's first portable MRI scanner, went on sale in the US in 2020, because of its unique design and ultra-low field of view (0.064T). The bi-planar, three-axis gradient system deployed in the point-of-care (POC) MRI has a peak amplitude of 26 mT/m and 25 mT/m, respectively Sheth K., et.al. (2021). Permanent magnet arrays that are smaller and lighter scan a greater volume encompassing organs like the skull. MRI imaging has employed permanent magnet arrays that provide dipolar magnetic fields. All these and many others open the possibility of building a genuinely portable, low-cost MRI scanner for brain imaging.

5. Conclusion and Future Work

The brain is one of the promising modalities to be posed as a biometric identification of an individual since human individuality entirely depends on the brain. The possible uniqueness of the visible structure of the brain which varies sufficiently from person to person has been explored here. The brain structure is comparatively stable over time than the brain's electrical signals in correspondence to various activities and behaviors and cannot be faked. To summarize, this paper achieves an important landmark to extract a secure and robust hidden biometric template in the form of a multipronged brain print. The generated template has been proven for uniqueness, scalability, irreversibility and security of template. We for the first time test the performance of the structural brain biometrics against the MRI intensity acquisition error of 5% and 10% pixels for which the accuracy of the system is 99.94% and FAR is 0 with negligible FRR. The brain structure has been optimized by using the multipronged angular transformed slices. The proposed multipronged brain print addresses the challenges of scalability, uniqueness, robustness against MRI acquisition noise and template security by creating a multipronged template containing optimal structural information and securing it with less processing and space complexity better in comparison with previous methods. The time taken for brain print creation is less than a second and the stored template size is less than 4KB per subject thus, the method enables real-time and portable applications. In future, we look forward to testing the proposed algorithm for portable brain imaging devices which may have different image formats and intensity contrasts so the method may be needed to adapt to become universally useful. For this, the proposed method needs to be tested on more subjects with a variety of brain imaging methods. Collaborations with some brain imaging centers can increase the scale of the testing.

Conflicts of Interest

The authors declare no conflict of interest.

References

- [1] Aloui, K.; Naït-ali, A.; Naceur, M.S. (2011): "New Biometric Approach Based on Geometrical Human Brain Patterns Recognition: Some Preliminary Results" IEEE.
- [2] Aloui, K.; Naït-ali, A.; Naceur, M.S (2011): "A novel approach-based brain biometrics: some preliminary results for individual identification." IEEE Workshop on Computational Intelligence in Biometrics and Identity Management (CIBIM)", pp. 91-95. IEEE.
- [3] Aloui, K.; A. Naït-ali, A.; Naceur, M.S.(2012): "A new useful biometrics tool based on 3d brain human geometrical characterizations".
- [4] Aloui, K.; Naït-ali, A.; Naceur, M.S (2018): "Using brain prints as a new biometric feature for human recognition." Pattern Recognition Letters 113, pp. 38-45.
- [5] Bassi, M.; Trivedi, P. (2018): "Human biometric identification through brain print," Second International Conference on Electronics, Communication and Aerospace Technology (ICECA). IEEE, pp. 1514–1518.
- [6] Bhatnagar, S.; Khandelwal, S.; Jain, N. (2013): "A Reconsideration of schemes for Fingerprint Identification." International Journal of Advanced Research in Computer Science 4, no. 3.
- [7] Bhatnagar, S. (2017): "Cooperative biometric multimodal approach for identification." In International Conference on Information and Communication Technology for Intelligent Systems, pp. 13-19. Springer, Cham.
- [8] Bhatnagar, S.; Mishra, N. (2020): "Conventional Biometrics and Hidden Biometric: A Comparative Study." In International Conference on Information and Communication Technology for Intelligent Systems, pp. 473-481. Springer, Singapore.
- [9] Bhatnagar, S.; Mishra, N. (2020): "A review of MRI brain print as hidden biometric," TEST Engineering & Management, vol. 83, p. 28571 – 28578.
- [10] Chen; Fanglin, et al. (2014): 'The potential of using brain images for authentication.' The Scientific World Journal.
- [11] Dubois; Julien; Adolphs, R. (2016): 'Building a science of individual differences from fMRI.' Trends in cognitive sciences 20.6, pp. 425-443.
- [12] Finn; Emily, S.; Scheinost, D.; Finn, D.M.; Shen, X.; Papademetris, X.; Todd Constable, R. (2017): "Can brain state be manipulated to emphasize individual differences in functional connectivity?" Neuroimage 160, pp. 140-151.
- [13] Maheshwari, S.; Choudhary, P. (2016): "Hidden biometric security implementation through human brain's artificial macro structure," Procedia Computer Science, vol. 78, pp. 625–631.
- [14] Sheth, K.N; Mazurek, M.H; Yuen, M.M; Cahn, B.A; Shah, J.T; Ward, A.; Kim, J. A.; Gilmore, E. J; Falcone, G.J.; Petersen, N. et al. (2021) "Assessment of brain injury using portable, low-field magnetic resonance imaging at the bedside of critically ill patients," JAMA Neurology, vol. 78, no. 1, pp. 41–47.
- [15] Takao; Hidemasa; Hayashi, N; Ohtomo, K. (2015): 'Brain morphology is individual specific information.' Magnetic resonance imaging 33.6, pp. 816-821.

- [16] Valizadeh; Abolfazl, S.; et al. (2018): 'Identification of individual subjects on the basis of their brain anatomical features.' Scientific reports 8.1, pp.1-9.
- [17] Rosen, V. J. W. B., A; Toga, W.: (2010), "Human connectome project (hcp) database," [Online]. Available: <https://ida.loni.usc.edu/login.jsp>
- [18] Wachinger, C; Golland, P.; Reuter, M. (2014): "Brainprint: Identifying subjects by their brain," in International Conference on Medical Image Computing and Computer-Assisted Intervention. Springer, pp. 41-48.
- [19] Wachinger, C.; Golland, P.; Kremen, W.; Fischl, B.; Reuter, M.; Alzheimer's Disease Neuroimaging Initiative. (2015): "BrainPrint: A discriminative characterization of brain morphology." NeuroImage 109, pp. 232-248.

Authors Profile



Shaleen Bhatnagar completed BE in Information Technology in 2009 and M.Tech. in Computer Science & Engineering in 2013 from Rajasthan, India. Currently, she is pursuing Ph.D. from Presidency University Bangalore India while working there as Assistant Professor. She has teaching experience of 11 years. Her research interests include Biometrics, Computer Vision, Pattern Recognition, Image Processing, and Machine Learning.



Dr. Aditya Kishore Saxena received the bachelor's degree in Computer Science from UP Technical University, in 2007. He has the master's degree in Information Security from IIIT Allahabad. He was awarded Silver Medal for securing an overall 2nd Position in the University. He completed Ph.D. degree from the Department of Computer Science, IIIT Allahabad, India, in 2017. He is presently working as Asst. Professor in Presidency University, Bangalore India. His research interests primarily focus on understanding how the behavior of individuals affects the overall mechanism of Biometric based authentication and classification.